DOI: https://doi.org/10.37434/tpwj2024.11.03

CORROSION-MECHANICAL STATE OF THE HEAT PIPELINE AFTER LONG-TERM OPERATION

P. Yukhymets[1], L. Nyrkova[1], R. Dmytriienko[1], H. Kaminski[2], C. Zaruba[2], P. Linhardt[2], G. Ball[2], V. Yehorenko[3]

[1]E.O. Paton Electric Welding Institute of the NASU
11 Kazymyr Malevych Str., 03150, Kyiv, Ukraine
[2]Technical University of Vienna. Karlsplatz 13, 1040 Vienna, Austria
[3]CE "Kyivteploenergo". 5 Ivan Franko Sq., 01001, Kyiv, Ukraine

ABSTRACT

Metal properties of heat pipeline areas thinned under operating conditions is necessary component for determining its real state, and therefore their research is an actual task. The work investigates the corrosion-mechanical state of a heating pipeline made of BSt3sp steel after more than 40 years of operation. Based on the conducted research, it was established that corrosion of the feeding pipeline is more severe than that of the return pipeline, while the external corrosion of the pipelines is more intense than the internal one. The cracking of the oxide layer accelerates with increasing stresses in the range of the design pressure and leads to the activation of corrosion processes and formation of through defects that prevents destruction by the mechanism of low-cycle fatigue. It is shown that tensile and yield strength of steel correspond to the minimum normalized values. The reduction in plasticity of the feeding pipeline metal does not exceed 10 %, while that for return pipeline is below the minimum normalized value which is probably due to strain aging. The least damaged layer adjacent to the inner surface of pipes has increased strength and plasticity characteristics due to the pipe manufacturing technology. While hydraulic test may not lead to the expected destruction at the location of through defects, its probability raises with increase of the test pressure.

KEYWORDS: heat pipelines, corrosion, mechanical properties, hardness, through defects

INTRODUCTION

Reliable operation of heat pipelines is vital for public safety, environmental protection and economic stability. The processes of general and local corrosion are among main factors of reducing the operational stability of pipelines of heat networks, strain aging, as well as deterioration of mechanical characteristics and resistance of metal to destruction. Corrosion leads to decrease in thickness of the pipe wall, origin of stress concentrators, decline in resistance to crack initiation and propagation, which can cause pipeline destruction at operation and test pressure [1, 2].

The real mechanical properties of the metal of the pipelines after long-term operation are necessary to assess their actual strength, residual life and investigation into the causes of failure. Experimental determination of the mechanical properties of pipe steels 19G and 17G1C after long operation in gas and oil pipelines revealed their minor changes [3]. At the same time, the question of the influence of long-term operation on the mechanical properties of structural materials of heat pipelines subjected to specific loads and impact of external and internal environment remains studied insufficiently. A characteristic feature of the pipelines of the heat network after long operation is the presence of local corrosion thinning, which is quite large in area and can eventually devolve into the category of critically thinned areas — where plastic deformations are observed at the hydraulic test pressure and below. Publications [4, 5] show the results of laboratory modeling of the heat pipeline operation. The obtained data on corrosion-mechanical properties made it possible to substantiate the low-cycle destruction of critically thinned areas and to provide recommendations on the pressure of periodic hydraulic tests of heat pipelines. Metal properties of areas thinned under operating conditions are one of the necessary components for determining their real state, and therefore their research is an actual task.

OBJECT OF RESEARCH

For conducting research were used two significantly corroded fragments, each ~2 m length, cut from feeding and return pipelines of the D325 main heating line laid in non-passable channel (Figure 1). Both fragments according to the results of periodic hydraulic test were recognized by the operating organization — KP Kyivteploenergo as unfit for further operation and transferred to PWI.

According to the technical documentation, the main heating line with design parameters of temperature T_d = 150 °C and internal pressure P_d = = 1.6 MPa was installed in 1976 using electrically welded heat-treated pipes 325×8 (external diameter × wall thickness, mm) manufactured from steel BSt3sp [6] (Tables 1–3) and covered with bitumen-pearlite insulation.

Figure 1. Feeding and return pipelines in a non-passable channel (*a*); through corrosion defects in the feeding pipeline (*b*)

Table 1. Chemical composition of the pipe metal

Source	Mass fraction of elements, %									
	C	Mn	Si	S	P	Cr	Ni	Cu	As	Mo
[5]	0.14–0.22**	0.40–0.65	0.12–0.30	<0.055	<0.045	<0.30	<0.30	<0.30	<0.08	–
Feeding pipe*	0.11	0.46	0.22	0.015	0.011	0.09	0.08	0.086	–	0.009
Return pipe*	0.11	0.47	0.22	0.018	0.012	0.09	0.08	0.090	–	0.009

*Results of spectral analysis of metal.
**Deviation from the lower limit of carbon content according to [6] is not a rejection sign.

For further investigation of the metal properties were selected the blanks from the thinnest parts of the feeding pipe (Table 3).

RESEARCH METHODS

CORROSION STATE

Visual control of the pipeline fragments was carried out according to [8], their corrosion condition was assessed according to [9].

Energy dispersive spectroscopy (EDS) microanalysis of oxide layer was conducted using scanning electron microscope Philips XL30 with EDAX Sapphire detector unit.

Experimental setup for investigation of influence of inner pressure on external corrosion included (Figure 2):

- blank No. 4 (Table 3);
- electrochemical cell made of acrylic glass tube glued to specimen surface (corresponding to pipe external surface) with acidfree silicone rubber glue in area with low number of visible defects in the oxide layer (as checked out under a microscope);
- electrolyte — $NaHCO_3$ solution prepared from deionized water with 500 mg/L HCO_3^-, chosen due to its relatively inert behavior in the corrosion of steel (not aggressive, not strongly inhibiting) and pH buffering effect, thus minimizing fluctuations in open circuit potential;
- silver-silver chloride electrode (SSE) reference electrode for continuous open circuit potential (OCP) measurement.

Continuous OCP measurement was used to detect the formation of cracks in the oxide layer during elongation test in steps of 200 N with a traverse speed of 0.1 mm/min and 2 min holding time. Stepwise elongation was performed to give OCP time of equilibration.

Table 2. Mechanical properties of pipes according to the certificate*

Source	σ_t^{wm}, MPa	σ_t, MPa	σ_{02}, MPa	δ, %
Certificate	438–465	441–456	–	32–38
[6]	–	372–480	245	26
[7]	>372	>372	>225	>22

*σ_t^{wm} — tensile strength of the of the welded joint metal; σ_t/σ_{02} — yield strength/conditional yield strength of the base metal; δ — relative elongation.

Table 3. Thickness of blanks

Nos	Minimum thickness (mm) of the left/right side edge of the blank
1	0.9/1.3
2	0.8/0.9
3	0.5/1.3
4	1.1/1.7
5	1.5/1.7
6	0.9/1.3

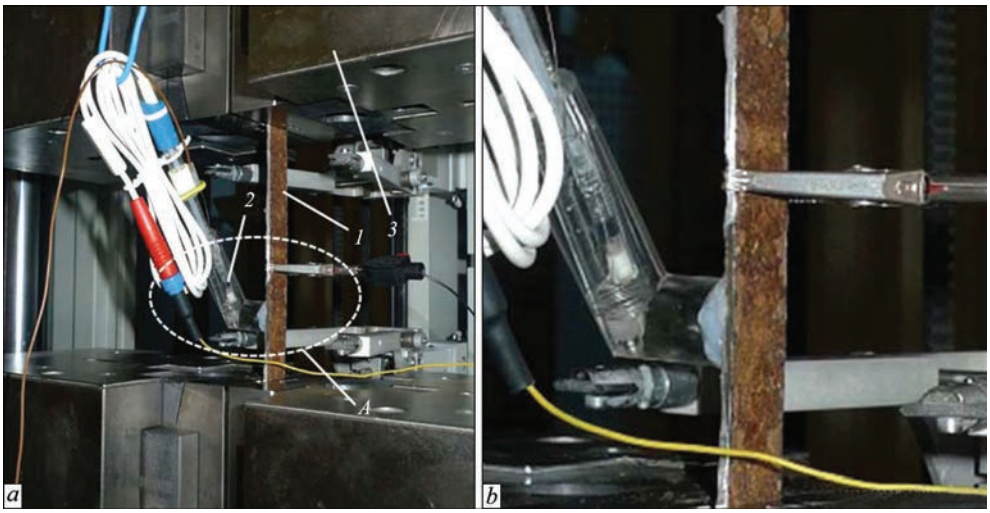

Figure 2. Corrosion experimental setup: *a* — *1* — blank No. 4; *2* — electrochemical cell filled with solution and SSE reference electrode; *3* — tensile machine traverse; *b* — *A* — enlarged

MECHANICAL PROPERTIES OF THE METAL OF THE ZONE WITH MINOR CORROSION DAMAGE

To study the mechanical properties of the metal (σ_t; $\sigma_{0.2}$, δ_5, ψ — relative narrowing of the cross-section) flat proportional samples $l_0 = 5.65\sqrt{F_0}$ with a thickness of 3 mm and width of the working part of 8 mm were made with mechanical processing of both surfaces in the thickness direction (Figure 3). The samples were cut out from the pipes in the circumferential and longitudinal directions. The places for the grips of circumferential samples before milling were straightened in the press in such way as not to deform the working part.

Mechanical tests were performed on the test machine MTS-318.25 with deformation rate 2 mm/min at temperature of ~22 °C, extensometer gauge length 25 mm, survey interval 0.1 s.

MECHANICAL PROPERTIES OF THE METAL OF THE MOST THINNED ZONE OF THE FEEDING PIPELINE

Tensile test of sample No. 3 (Figure 4, *a*) made from blank No. 3 (see Table 3) was performed on Zwick Z050 testing machine according to [10] with a deformation rate of 1.25 mm/min at temperature ~23 °C, extensometer gauge length 40 mm, the survey interval 0.02 s. Mechanical properties metal (σ_t, σ_{02}, δ_5, ψ) were determined on the base of test results.

Tensile testing of samples (Figure 4, *b*) made from blank No. 1 (see Table 3) was carried out at a constant room temperature using a dilatometer. For definition of tensile strength σ_t and yield strength σ_{02} of the material were used shorter samples, which made it possible to optimize the volume of mechanical processing.

LOW FORCE HV HARDNESS

Vickers hardness measurements *HV*1, *HV*0.3 were carried out according to [11] using hardness tester EMCO Test M1C 010 and CARL ZEISS Axio Imager.M2m microscope.

GRAIN SIZE

The grain size of ferrite and pearlite in the hardness measurement area was defined using CARL ZEISS Axio Imager.M2m microscope at magnification 500:1 according to [12].

RESULTS OF EXPERIMENTS AND THEIR ANALYSIS

The results of visual inspection proved that both pipes: feeding and return are single-seam, welded

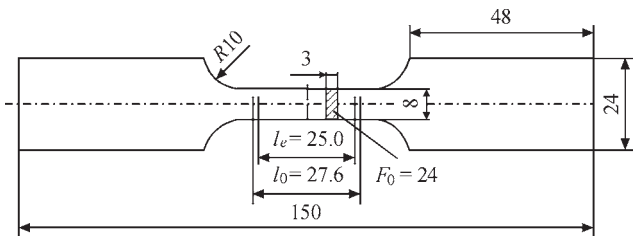

Figure 3. Sample for tensile tests: l_e — extensometer gauge length; l_0 — original gauge length; F_0 — original cross-sectional area

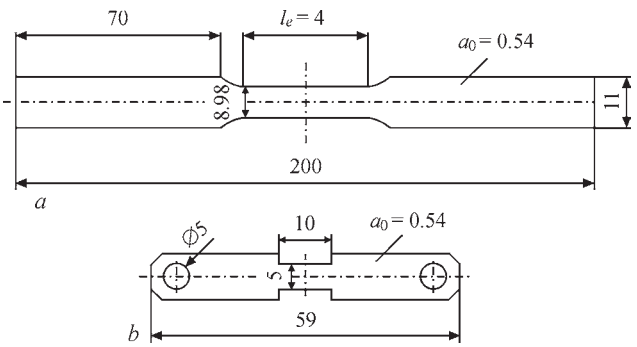

Figure 4. A sample for tensile testing of the metal of the thinnest zone: *a* — on a tensile machine; *b* — on the dilatometer; l_e — extensometer gauge length

with high-frequency currents. At the time of inspection protective cover is practically absent. The outer surface of both pipes is covered with a layer of brown corrosion products, there are remnants of a protective coating, probably bituminous. Local corrosion damage detected on the surface of the pipes identified according to [9] as corrosion spots and pits of various sizes. The inner surface is covered with a layer of brown corrosion products that are easily separated from the pipe wall and fall apart. Corrosion of the inner surface is continuous and uniform. The corrosion state of the pipe fragments is unsatisfactory, while the corrosion damage of the feeding pipe is more significant. The thickness of the wall of the feeding pipe is unevenly reduced, probably due to corrosion, in the range from 7–8 to 1–2 mm; the thickness of the remains of the protective cover is 280–470 μm. Visually, the pits on the outer surface have a greater depth than on the inner surface — it should be assumed that the outer corrosion is more intense than the inner one. Corrosion pits on the outer surface vary in size: from 3×3 mm to 25×50 mm; in the region of the smallest wall thickness three through corrosion defects with dimensions of ~7×5, 6×5 and 13×7 mm were found (see Figure 1, *b*). Corrosion destruction probably started from side of the outer surface. Wall thickness of the return pipe varies from 7–8 mm to 3–4 mm, the thickness of the remains of protective cover is 0.25–6.7 mm.

Figure 5 shows the results of EDS microanalysis of the oxide layer of the feeding pipeline. As can be seen, the main component of the layer is iron, presumably in the form of FeO and Fe_2O_3 oxides, which were formed as a result of the electrochemical reaction between iron and water.

The potential of the open circuit turned out to be quite sensitive to the cracking of the protective layer. During the entire tensile time of the sample, a potential shift from –0.527 to –0.565 V, which indicated the loss of the protective properties of the oxide layer, presumably due to cracking and peeling. Under elastic deformation by tensile force in range $0 < S < 1200$ N (taking into account the thickness of the cross-section of the blank at the location of the electrochemical cell ~2 mm this corresponds to the pressure $0 < P < 0.5$ MPa in the pipeline D325) the potential almost did not change and reached –0.523 V. Further increase of tensile force up to 3000 N caused decease of OCP by about 5–7 mV, but with an increase in the force from 3000 to 4000 N, a sharp shift of the potential from –0.530 to –0.555 V was noted, which is due to the formation of areas of freshly exposed metal.

A synopsis of force and OCP over time (Figure 6) shows that there is a critical elastic load $S \sim 3000$ N (corresponding to an internal pressure $P \approx 1.3$ MPa),

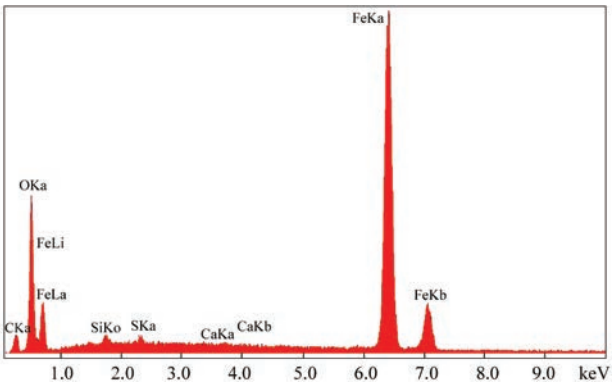

Figure 5. EDS spectrum of the oxide layer on the surface of feeding pipe

where the OCP rapidly decreases with each subsequent increase in tension. This indicates the beginning of the formation of deep cracks in the oxide layer, which significantly activate local corrosion processes.

The synopsis of force and OCP over time (Figure 6) reveals that there is a critical elastic load $S \sim 3000$ N (which corresponds to the internal pressure $P \approx 1.3$ MPa in the D325 pipeline with a thickness of $a = 2$ mm in the thinning zone), where OCP decreases rapidly and instantaneously with each further step in force. This indicates the onset of formation of deep cracks in the oxide layer, activating corrosion processes to a significant degree.

However, OCP provides no quantitative information on the corrosion processes induced by such cracking. On the other hand, the true quantitative effect in practice is hardly accessible by laboratory experiments as it depends on a large number of parameters occurring in the real environment (presence of humidity or liquid water, chemical composition of the water, possible galvanic effects in the system, wet-dry-cycles, etc.).

The results of visual inspection and OCP measurements satisfactory agree with the data of corrosion-mechanical tests of 17G1S steel from D630 pipe [5], according to which:

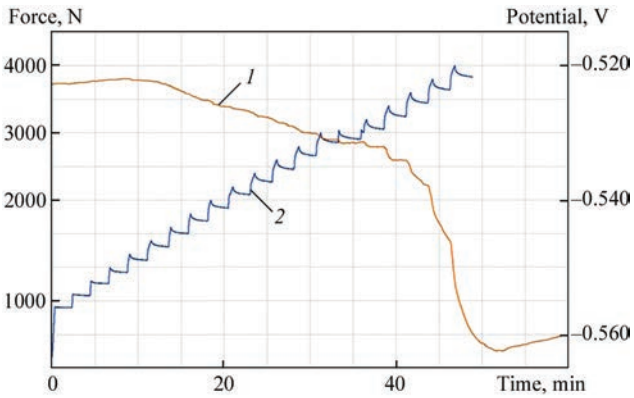

Figure 6. Change in the potential of the open circuit (*1*) of the sample under applied tensile force (*2*)

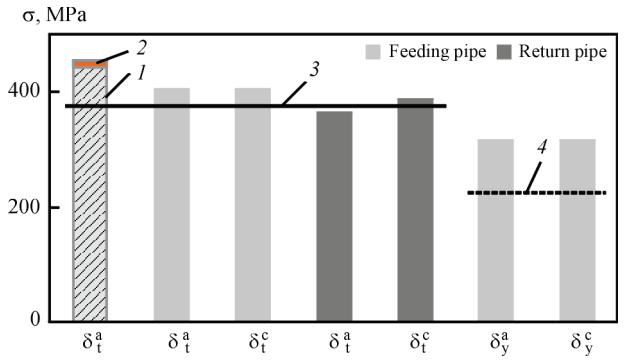

Figure 7. Tensile (σ_t) and yielding (σ_{02}) strength of metal of feeding and return pipes; upper indexes: *a* — axial direction; *c* — circumferential direction. *1* — certificate data; *2* — range of values; *3*, *4* — minimal values of σ_t, σ_{02} according to [7], correspondingly

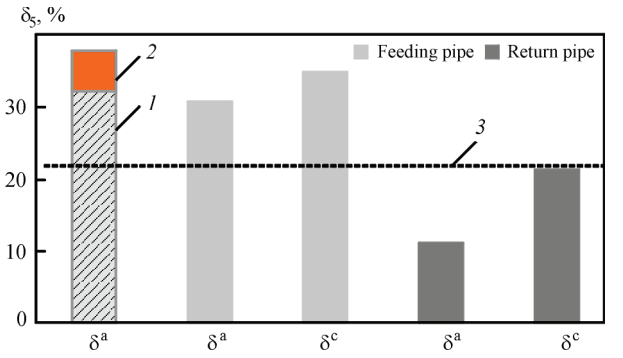

Figure 8. Elongation after fracture δ_5 of metal of feeding and return pipes; upper indexes: *a* — axial direction; *c* — circumferential direction. *1* — certificate data; *2* — range of values; *3* — minimal value of δ_5 according to [7]

● at temperature of 80 °C (average operating temperature of feeding heat pipeline) the corrosion rate is twice higher than at a temperature of 40 °C (average operating temperature of a return pipeline);

● the corrosion process is accelerated as the working pressure increases (the internal pressure in feeding pipeline is ~2 times higher than in a return pipeline) and becomes more substantial when the stresses periodically attain the level corresponding to the pressure of hydraulic tests (P = 2 MPa).

Comparing of the results of tensile tests with the data of the certificate (Figures 7, 8) shows that after long-term operation (more than 40 years), the value of tensile strength in the axial direction σ_t^a of material of feeding pipeline decreased by ≈10 % and return pipeline by ≈18 %. Strength characteristics σ_t and σ_{02} of metal of feeding and return pipelines in circumferential and axial directions are practically the same and meet the minimum requirements of regulatory documentation, that generally agrees with the results [4] obtained in the absence of residual deformation. Reduction in plasticity of material of feeding pipeline in circular and axial direction does not exceed 10% and meets requirements [7]. Decrease in plasticity of material of return pipeline is more significant, especially in longitudinal direction, where it is lower than the minimum regulatory value by ≈50 % which is probably a consequence of strain aging in the conditions of local bending of the pipeline and increases the susceptibility to brittle failure, including under explosive loading.

Results of tensile tests on material of feeding pipeline are given in Table 4 and Figure 9.

The increased strength and plasticity characteristics of the material of the significantly thinned zone of the pipe are explained by selection of samples No. 3, D1-1, D1-2 for tensile tests from the least damaged layer adjacent to the inner surface of the pipe, the properties of which are specific due to the pipe manufacturing technology, as well as the influence of scale factor (the thickness of the samples differs by ~6 times).

The trends of hardness change across thickness of blanks Nos 4 and 6 (Figure 10, *c*) agree with the results (Table 4.) The increase in hardness near the inner surface of the pipe indicates technological strengthening of the metal during the pipe manufacturing process, as well as the insignificance of internal corrosion. The hardened near-surface layer on the outside, apparently due to more intense corrosion, was not preserved.

Stated above can be confirmed also by the results of grain size measurements (Figure 11). The average grain size near the inner surface of the pipe is ≈2 (blank No. 6)

Table 4. Mechanical properties of material of feeding pipeline in axial direction

Specimen No.	1	3	D1-1	D1-2
Test machine	MTS	Zwick	Dilatometer	
Location	Minor corrosion	Significant corrosion thinning		
σ_t, MPa	408.0	442.1	449.7	443.7
σ_{02} MPa	320.0	333.1	338.3	333.2
δ_5, %	30.8 (l_e = 25 mm)	23.70 (l_e = 40 mm)/37.8*	–	–
ψ, %	56.4	73.8	–	–

*Value of relative elongation δ_5 = 37.8 % of the non-proportional sample 3 was calculated according to [13] for comparison with the relative elongation of the proportional sample 1.

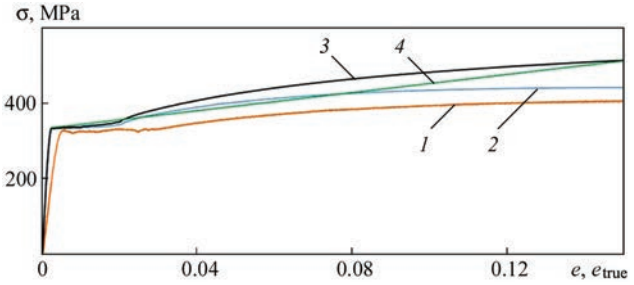

Figure 9. Tensile stress diagrams of samples Nos 1 and 3 within the limits of uniform thinning; *1* — specimen No. 1, regular diagram ($e = \Delta l_e / l_e$ (l_e — initial calculated length according to the strain gauge, Δl_e — elongation of initial calculated length according to the strain gauge), $\sigma = S/F_0$, (S — tensile force; F_0 — area of specimen cross-section); *2* — specimen No. 3, regular diagram; *3* — true stress-strain diagram of specimen No. 3 ($e_{true} = \ln(1 + e)$; $\sigma_{true} = \sigma(1 + e)$); *4* — approximated bilinear hardening diagram of specimen No. 3

and 10 % (blank No. 4) smaller than in the middle part of the cross-section across the thickness.

In Figure 12 are shown the results of hardness measurements in the zone of significant thinning of No. 4 blank, performed on the side face (in the direction of maximum tensile stresses caused by internal pressure). Despite the fact that the minimum thinning thickness $a_{min} = 0.68$ mm is significantly lower than the threshold value of the thickness $a_{max}^{CTA} = 0.97$ mm, which is calculated by substituting the mechanical properties of sample No. 1 (Table 4) in (1) and determines the beginning of the plastic deformation of the pipeline wall at the pressure of hydraulic tests $P = 2$ MPa:

$$a_{max}^{CTA} = \frac{PD_0}{2\left(\sigma_{02} + \frac{P}{2}\right)} \quad (1)$$

the obtained values are practically the same in the middle of the thickness and in the near-surface layers of the metal. This indicates the absence, as a result of intensive corrosion of the original technologically strengthened layers of the outer and inner surfaces, as well as the absence of accumulated residual deformations, which is confirmed by FEA calculations and measurements of the hardness on the side surface of the sample after tensile test.

The dimensions of a fragment of the longitudinal section of the supply pipeline D325 were used to construct the geometric model of the pipeline (Figure 12, *a*). Modeling of defects on the surface of the pipe was carried out by rotating the corresponding complementary segments around the axes located coaxially with the pipe (Figure 13). The thickness of the pipe $a = 2$ mm approximately corresponds, according to visual inspection, to the average value of the wall thickness of adjacent sections in the area where the specified fragment of the longitudinal section is located. The true tensile diagram of sample No. 3 (Figure 9), approximated by the bilinear method

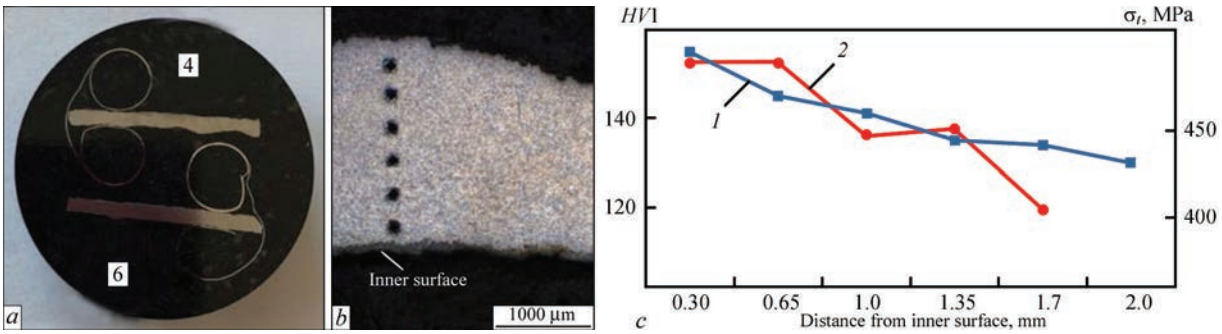

Figure 10. Measurement of hardness along the wall thickness of a pipe with significant corrosion thinning: *a* — measurement template, the numbers indicate the blank numbers (see Table 3); *b* — specimen from blank No. 4 after indentation; *c* — hardness *HV*1 and tensile strength σ_t across the thickness of the specimens No. 4 (1) and No. 6 (*2*); calculation of σ_t values according to [11]

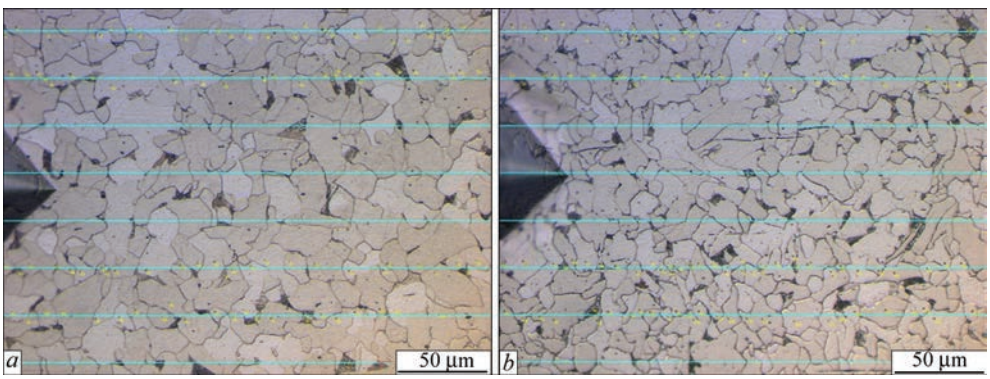

Figure 11. Measurement of grain size of sample No. 4 at the: *a* — middle of wall thickness; *b* — near the inner surface

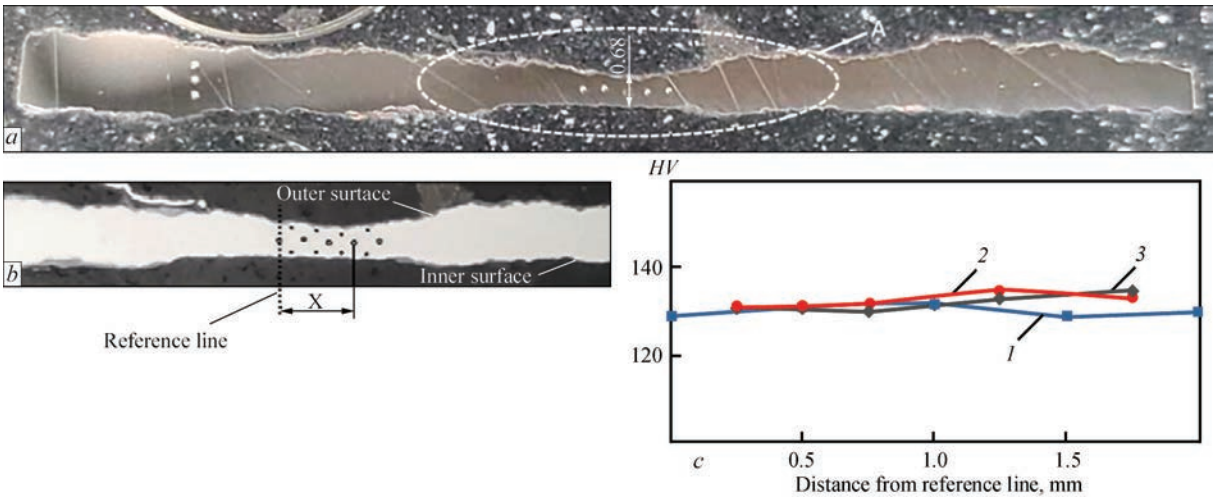

Figure 12. Measurement of hardness along the thickness of a significantly thinned wall: *a* — template after *HV*1 measurements; *b* — zone A after *HV*1 and *HV*0.3 measurements; × — distance from the reference line to the measurement point; *c* — hardness along wall thickness: *1* — middle of the thickness, *2* — outer surface; *3* — inner surface

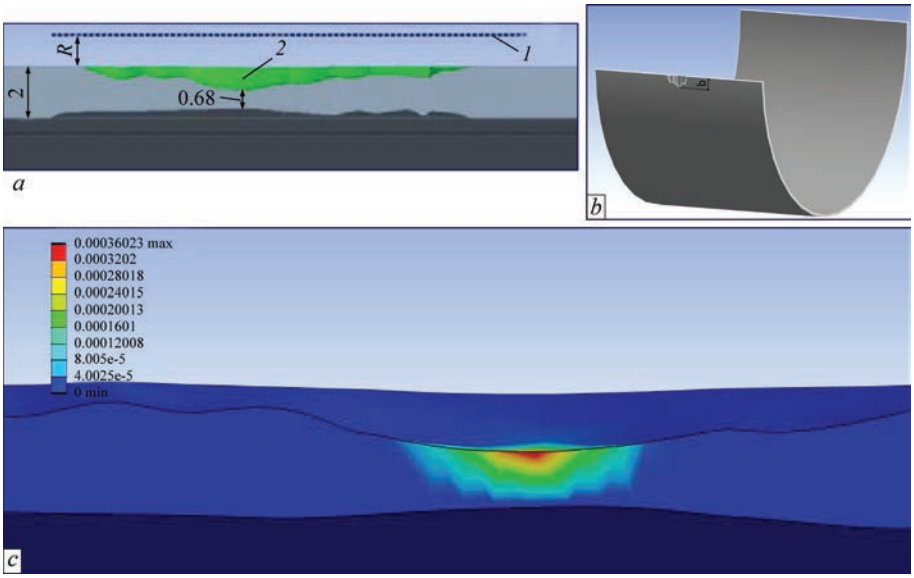

Figure 13. Model defect: *a* — application scheme: *1* — axis of rotation; *2* — complementary segment, *R* — radius of rotation; *b* — defect on outer surface (*b* — half width of defect); *3* — distribution of plastic strains

(σ_{02} = 334 MPa, σ_t = 516 MPa, tangential modulus G_t = 1200 MPa), was used in the calculation. Table 5 presents the maximum plastic deformations of three defects with different geometric parameters under the hydraulic test pressure P = 2 MPa. Relatively low values of the maximum deformations on the outer surface in the zone of greatest thinning are a consequence of unloading bending caused by the action of internal pressure.

The results of Vickers hardness measurement under a load of 0.3 kg (*HV*0.3) on the side surface of sample D1-1 after its tensile test are shown in Figure 14.

Table 5. Maximal plastic strain *e* in defect

Variant No.	Radius *R*, mm	Width *b*, mm	$e \cdot 10^{-2}$, %
1	3	2.5	0.07
2	50	8.2	4
3	100	11.4	10

The approximate value of residual plastic deformation e_r at the *i*-th point of hardness measurement was determined as

$$e_{ri} \approx \ln\left(\frac{a_0}{a_i}\right),$$

where a_0 — initial thickness of the cross-section of the sample; a_i — thickness of the cross-section of the sample at the *i*-th point after testing.

The given data (Figure 14, *c*) confirm that the values of the maximum plastic deformations $e_r < 0.1$ % of the template with the minimum thickness a_{min} = 0.68 mm do not significantly affect the hardness.

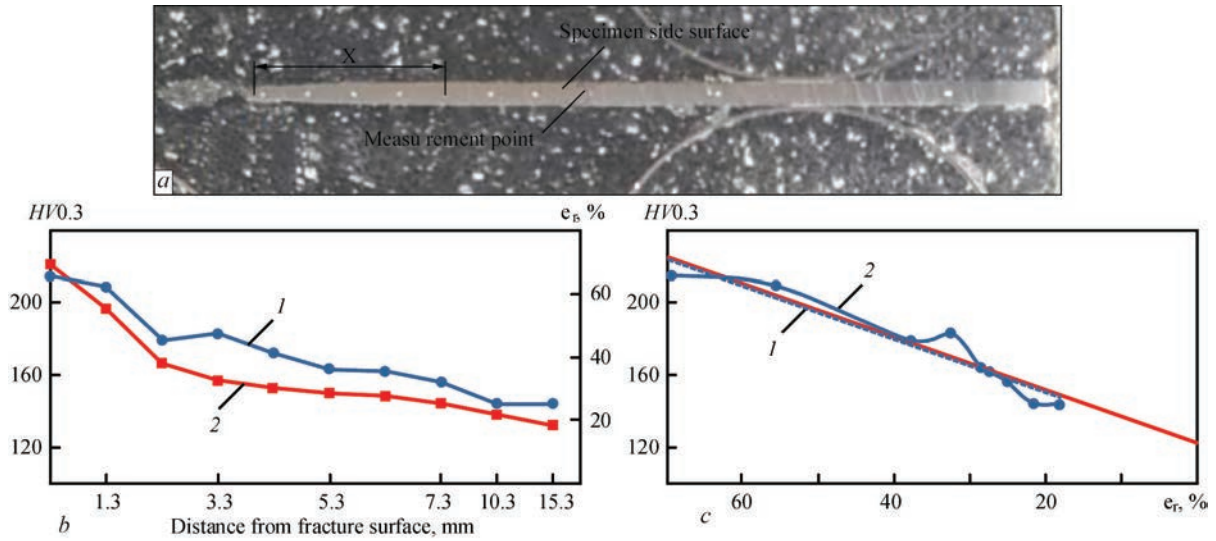

Figure 14. Hardness along the length of the side surface of sample D1-1 after tensile testing: *a* — side surface of the sample; × — the distance of the measurement point from the fracture surface; *b* — results of hardness measurement (*1*) as a function of the distance from the fracture surface and residual plastic deformation e_r (*2*); *c* — linear approximation of hardness values *HV* (*1*) depending on residual deformation e_r (*2*)

Further decrease in the thickness of the pipe and wall can lead to an increase in the rate of corrosion due to an increment in the operating stresses and residual plastic deformation. At the same time, under the influence of variable operating loads, accumulated low-cycle damage occurs in the surface layer of the most thinned areas and corrosion pits [4]. The presence of through corrosion defects indicates that, due to the fast development of wall corrosion, accumulated fatigue damage in the constantly renewed surface layer does not have time to reach a critical value.

Evaluation of the strength in the presence of through-hole defects, can be done using hypothesis according to which the bearing capacity of the pipeline will decrease if:

$$A_d > A_0,$$

where A_d — the longitude cross-sectional area of the weakening caused by defect; A_0 — longitudinal cross-sectional area of the maximum round hole, which does not reduce bearing capacity of the pipeline.

According to [14] for pipe 325×8:

$$A_0 = d_0^{P_b} a = 100.8 \text{ mm}^2,$$

where $d_0^{P_b}$ — max diameter of the round hole at burst pressure P_b of the pipe:

$$d_0^{P_b} = 0.25\sqrt{D_m a},$$

where D_m — average diameter of the pipe; a — nominal pipe thickness.

For assessment of strength of the considered fragment of feeding pipeline let's schematize through de-

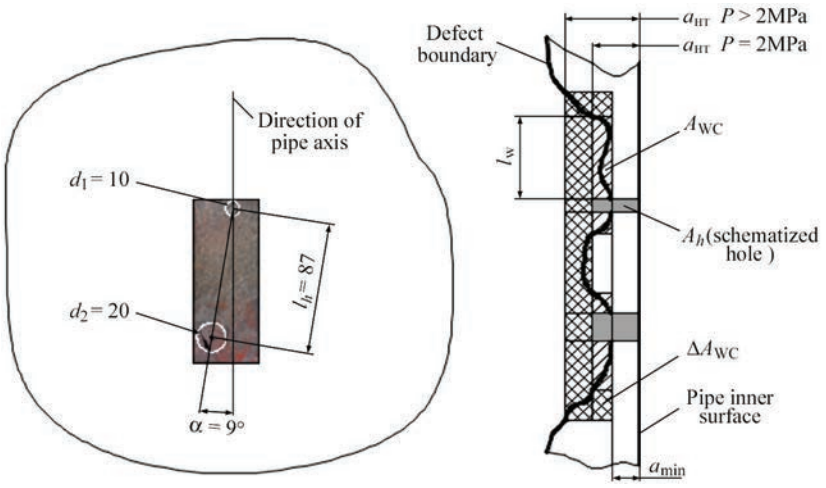

Figure 15. Schematization of through hole defects: *a* — top view: d_1, d_2 — diameters of defects circumscribing holes; *b* — calculation scheme: a_{HT} — minimal allowable thickness under pressure P; l_W — length of adjacent weakened zone; a_{min} — minimal remain thickness; A_{WC} — calculated area of adjacent weakened zone; A_h — area of schematized hole; ΔA_{WC} — increase of weakened area

fects by circumscribing holes with diameter d_1 and d_2 (Figure 15, *a*). As far as (Figure15, *b*):

$$l_d < 2\sqrt{D_m a} \text{ and } \alpha < 15°$$

we will consider these holes as lying in the same cross-section and belonging to the same defect of complex shape. Since no destruction occurred during the hydraulic test (P = 2 MPa), it can be stated in relation to the specified defect that:

$$A_d = \sum A_h + \sum A_{WC} < A_0,$$

where A_h — area of schematized hole:

$$A_h = da_{\text{HT}},$$

where d — diameter of circumscribing hole; a_{HT} — minimal allowable thickness during hydraulic test according to (1); A_{WC} — calculated area of longitudinal cross-section of adjacent to hole zone with remaining thickness less then a_{HT}:

$$A_{WC} = \left(a_{HT}^{P} - a_{min}\right) l_W,$$

where a_{min} — minimal remain thickness of defect excluding through holes; l_W — length of longitudinal cross-section of adjacent to hole zone with remaining thickness less than a_{HT}.

Thus, hydraulic test does not guarantee planned destruction of the pipeline in the presence of relatively small through defects. Accordingly, the insignificant leakage of water caused by them, makes it difficult their detection, especially when pipeline lays in an impassable channel.

It should be noted that at the time of conducting hydraulic test information on the presence of through defects and their characteristic geometric parameters, as a rule, is not available, therefore preliminary determination of the destructive pressure of the damaged pipeline is impossible. At the same time with an increase of the test pressure the probability of failure of pipeline with through defects become large due the raising of weakened area ΔA_{WC} (Figure15, *b*).

CONCLUSIONS

Based on the conducted research, it was established that after long-term operation of the heat pipeline:

- Corrosion state of the heat pipelines is unsatisfactory. The protective coating does not meet the requirements of regulatory documents in terms of physical and mechanical indicators. The damage of the feeding pipeline, which was subjected to more significant operational loads, is more severe than that of the return pipeline, while the external corrosion of the pipelines is more intense than the internal one.
- Cracking of oxide layer, which begins in most thinned areas and in corrosion pits of feeding pipeline, accelerates with increasing stresses in the range of the design pressure, which leads to the activation of corrosion processes and formation of through defects that prevents destruction by the mechanism of low-cycle fatigue.
- Value of the tensile strength of the structural material (BSt3sp) of the feeding pipeline decreased by ≈10 %, return pipeline by ≈18 %. Tensile and yield strength of the pipeline material in the circumferential and axial direction are practically the same and correspond to the minimum normalized values. Reduction in plasticity of the material of feeding pipeline does not exceed 10 %, while that for return pipeline is more significant, especially in the axial direction, where it is below the minimum normalized value which is probably due to strain aging and increases the tendency to brittle failure.
- Increased strength and plasticity characteristics of the material of significantly thinned areas are caused by the selection of tensile samples from least damaged layer adjacent to original inner surface, the properties of which are specific due to the pipe manufacturing technology, as well as influence on results of the scale factor of used for comparison specimens.
- Hydraulic test may not lead to expected destruction at the location of through defects, depending on the geometric parameters of damage, which, given relatively small size of defects and accordingly insignificant leakage of water, makes it difficult to detect them when pipeline lays in an impassable channel.

REFERENCES

1. Torop, V.M. (2022) Conducting hydraulic tests of pipelines of heat networks in order to achieve the specified reliability of their operation. *Tekh. Diahnost. ta Neruiniv. Kontrol*, **3**, 35–41 [in Ukrainian].
2. Pleshivtsev, V.G., Pak, Yu.A., Pak, Yu.A., Filippov, G.A. (2008) Factors that reduce the structural strength of pipe metal and the prospects for creating new pipe steels for heating networks. In: *Proc. of 3rd Sci.-Pract. Conf. on Heat Networks. Modern Practical Solutions* [in Russian]. www.rosteplo.ru/Tech_stat/stat_shablon.php?id=2076pov
3. Penkin, A.G., Terentyev, V.F., Maslov, L.G. (2004) *Assessment of the degree of degradation of mechanical properties and residual service life of pipe steels using acoustic emission and kinetic hardness methods* [in Russian]. //www.sds.ru/articles/degradation/index.html
4. Yukhymets, P.S., Dmytryenko, R.I., Palienko, O.L., Yegorenko, V.M. (2022) Mechanical properties of the metal of critically thinned sections of the heat pipe and features of their destruction. *Tekh. Diahnost. ta Neruiniv. Kontrol*, **4**, 34–46 [in Ukrainian].
5. Yukhymets, P.S., Nyrkova, L.I., Gopkalo, O.P. (2022) Specific features of corrosion heating network pipelines made of 17G1S steel. *Materials Sci.*, 58(**1**), 35–40.
6. (2005) GOST 380: *Carbon steel of ordinary quality. Brands.*
7. (1980) GOST 10705: *Electric-welded steel pipes. Technical Conditions*.
8. (2005) DSTU EN 13018: *Non-destructive testing. Visual control. General requirements*.

9. (1985) GOST 9.908: *Unified system of protection against corrosion and aging. Metals and alloys. Methods of determining corrosion indicators and corrosion resistance.*
10. (2009) DIN EN ISO 6892-1: *Metallic materials — Tensile testing — Pt 1: Method of test at room temperature.*
11. (2018) ISO 6507-1: *Metallic material. Vickers hardness test. Pt 1: Test method*.
12. (2024) ASTM E112: *Standard test methods for determining average grain size***.**
13. (1999) EN ISO 2566-1: *Conversion of elongation values. Pt 1: Carbon and low alloy steels.*
14. (1986) PNAE G-7-002: *Standards for calculation of strength of equipment and pipelines of nuclear power installations.*

ORCID
P. Yukhymets: 0000-0002-8824-9024,
L. Nyrkova: 0000-0003-3917-9063
R. Dmytriienko: 0000-0001-8842-5051
P. Linhardt: 0000-0002-4523-2185

CONFLICT OF INTEREST
The Authors declare no conflict of interest

CORRESPONDING AUTHOR
P. Yukhymets
E.O. Paton Electric Welding Institute of the NASU
11 Kazymyr Malevych Str., 03150, Kyiv, Ukraine.
E-mail: yupeter@ukr.net

SUGGESTED CITATION
P. Yukhymets, L. Nyrkova, R. Dmytriienko, H. Kaminski, C. Zaruba, P. Linhardt, G. Ball, V. Yehorenko (2024) Corrosion-mechanical state of the heat pipeline after long-term operation. *The Paton Welding J*., **11**, 20–29.
DOI: https://doi.org/10.37434/tpwj2024.11.03

JOURNAL HOME PAGE
https://patonpublishinghouse.com/eng/journals/tpwj

Received: 12.09.2024
Received in revised form: 14.10.2024
Accepted: 02.12.2024